

RESEARCH ARTICLE

Editorial Process: Submission:05/07/2024 Acceptance:02/06/2025

High *APEX1* Expression Facilitates Osteosarcoma Cell Proliferation

Yan Yu Lu, Wen Lu, Jie Zheng, Ju Shu Luo*

Abstract

Osteosarcoma (OS) is a serious malignancy affecting children and young adults; however, there is limited improvement in the survival of patients with OS over the past four decades. Molecular targeted therapy is a promising treatment strategy for OS. Apurinic/aprimidinic exonuclease 1 (*APEX1*)-a key factor for DNA damage repair-is associated with OS proliferation, but the underlying molecular mechanism remains unclear. *APEX1* expression in OS tissues and paired paracancerous tissues and in human osteoblast cell line hFOB1.19 and OS cell lines was determined using real-time quantitative PCR (RT-qPCR). *APEX1*-shRNA and NC-shRNA lentiviral vectors were constructed and transfected into MG-63 cells. The effects of *APEX1* knockdown on MG-63 cell proliferation and apoptosis were assessed using MTT, xenograft tumor growth, and terminal deoxynucleotidyl transferase dUTP nick end labeling assays. Expression changes of apoptosis- and angiogenesis-related genes due to *APEX1* knockdown were detected using RT-qPCR and immunohistochemistry. To preliminarily determine the mechanism by which *APEX1* affects OS cell proliferation, transcription factors were predicted using three databases, and construction of protein-protein interaction network, gene ontology and Kyoto Encyclopedia of Genes and Genomes pathway enrichment analyses were performed. *APEX1* expression was higher in OS tissues than in paracancerous tissues. *APEX1* expression was also higher in OS cell lines than in hFOB1.19 cells, with the highest *APEX1* expression observed in MG-63 cells. *APEX1* knockdown mediated by *APEX1*-shRNA lentivirus markedly suppressed MG-63 cell proliferation both in vitro and in vivo and induced their apoptosis. *APEX1* knockdown downregulated CD31 expression but had no effect on the expression of P53 and Caspase3. Bioinformatics analyses suggested that USF1 or SP1 regulates *APEX1* transcription and its recruitment in DNA damage response pathways, affecting OS cell proliferation. Thus, high *APEX1* expression in OS facilitates cell proliferation likely via CD31, and USF1 or SP1 may regulate *APEX1* transcription and its recruitment in DNA damage response pathways.

Keywords: Apurinic/aprimidinic exonuclease 1- Osteosarcoma- Tumor proliferation- DNA damage response

Asian Pac J Cancer Prev, 26 (2), 453-463

Introduction

Osteosarcoma (OS) is the most common primary malignancy of bone, and its average annual incidence rate for all racial groups is approximately 4.4 cases per million individuals (1). OS has been reported at all ages but displays a bimodal distribution of incidence, with the majority of cases occurring in the second decade of life and a second peak incidence observed among adults aged >65 years, usually as a consequence of Paget disease [1]. OS is characterized by rapid progression, high metastasis potential, and poor clinical prognosis. The key factors affecting the prognosis of patients with OS include tumor size and location, distant metastasis, surgical margins, and response to chemotherapy. The 5-year overall survival of patients with OS has been close to 70% [2], but most cases are initially classified as Enneking Stage IIB; moreover, 10%–20% of patients present with pulmonary

metastasis, and their 5-year survival rate remains less than 30% [3]. The current challenges in the treatment of OS include the high mortality of patients with recurrence or metastasis and the stagnation in survival improvement over the past few decades. The difficulties in evidence-based medical research for OS result from the extreme complexity of genetic characteristics [4-7], diversity in tumor microenvironment [8], chemotherapeutic drug resistance, pulmonary metastasis, and low incidence, owing to which the clinical efficacy of OS has reached a plateau. Therefore, research on precision targeted therapy for OS based on genomics holds the key for making a breakthrough in OS clinical treatment.

APEX1 is a multifunctional protein. The gene encoding *APEX1*, is located on chromosome 14q11.2, spans 15 kb, and contains five exons. *APEX1*, with a molecular weight of approximately 35.6 kDa, is mainly located in the nucleus and mitochondria. *APEX1* is a key enzyme

Division of Spinal Surgery, The First People's Hospital of Yulin (The Sixth Affiliated Hospital of Guangxi Medical University), No. 495 Mid-way of education, Yulin, 537000, Guangxi, China. *For Correspondence: m13457691460@163.com

involved in repairing the DNA damage caused by oxidant and alkylating agents that produce cytotoxic and genotoxic apurinic/apyrimidinic sites. Failure to repair the DNA damage may lead to mutation, chromosomal instability, and cell apoptosis [9]. Moreover, *APEX1* maintains certain intracellular transcription factors (TFs) in a reduced state through its reduction–oxidation and thus participates in oxidative stress, transcriptional regulation, cell cycle progression, proliferation, differentiation, and apoptosis. Notably, cancer-related TFs such as *p53*, *NF-κB*, *Myb*, *PAX*, *HIF-1*, *Egr-1*, *CREB*, and *AP-1* are reported to be regulated by *APEX1* [10–12].

Dysregulated expression of *APEX1* has been demonstrated in several cancers. Increased expression of cytoplasmic *APEX1* is associated with shorter disease-free survival and is a predictor of relapse in patients with hepatocellular carcinoma and cholangiocarcinoma. Serum *APEX1* is a potential diagnostic biomarker of clear cell renal cell carcinoma, hepatocellular carcinoma, and cholangiocarcinoma [13, 14]. Additionally, the regulatory function of *APEX1* in cholangiocarcinoma metastasis may be mediated by cell division cycle 42 (*CDC42*) and son of sevenless homolog 1 (*SOS1*) [15]. Downregulated expression of *APEX1* has been demonstrated to repress cell proliferation, invasion, and migration and induce apoptosis in hepatocellular carcinoma cell lines through *MAP2K6* [16]. *APX2009*, a specific *APEX1* redox inhibitor, was reported to decrease the proliferative, migratory, and invasive potential of breast cancer cells. In contrast, upregulated expression of *APEX1* reduced the proliferation and induced the apoptosis of non-small-cell lung cancer (NSCLC) cells by regulating aberrant alternative splicing of key tumorigenic genes involved in the *MAPK* and *Wnt* signaling pathways [17]. These findings suggest that *APEX1* is closely associated with the biological behavior of malignant cells.

Upregulation of *APEX1* expression observed in OS tissues was found to be associated with OS recurrence and metastasis, which was demonstrated to be an independent predictor of disease-free survival in patients with OS. Moreover, *APEX1* knockdown suppressed U2-OS cell proliferation by downregulating *NF-κB* [18, 19]. *APEX1* is reported to be involved in OS angiogenesis through the regulation of the *TGF-β/Smad3* signaling pathway [20]; similarly, it has been reported that OS angiogenesis is associated with *FGF2* and *FGFR3* expression, which is regulated by *APEX1* [21]. Another study found that the overexpression of microRNA-135a downregulated *APEX1* to inhibit OS cell migration, proliferation and invasion and promoted cell apoptosis [22]. In addition, mitochondrial *APEX1* overexpression reduced the reactive oxygen species (ROS) production by decreasing *Rac1* phosphorylation, further enhancing cisplatin resistance in OS [23]. Research suggests that high *APEX1* expression indicates a poor clinical outcome for patients with OS and *APEX1* knockdown increased the sensitivity of OS cells to radiotherapy, chemotherapy drugs, and tumor angiogenesis inhibitors [24]. *APEX1* redox activity inhibition sensitized OS cells to ionizing radiation by inducing ferroptosis [25]. Some miRNAs have been shown to target *APEX1*, leading to decreased resistance

to chemoradiotherapy [26–28]. Notably, the promoters of genes encoding microRNAs that are downregulated as a result of *APEX1* knockdown harbor binding sites for several cancer-related transcription factors such as *NF-κB*, *p53*, *HIF-1α*, *AP-1*, *PEBP2*, *ATF*, *NF-Y*, *Pax-2*, *CREB*, and *c-Myb* [29]. Thus, *APEX1* may regulate the expression of those miRNAs by regulating the activity of these cancer-related TFs, subsequently affecting the biological behavior of OS cells.

The aim of this study was to explore the role of *APEX1* in OS cell proliferation. For this purpose, we assessed *APEX1* expression in human OS tissues and adjacent tissues, as well as in the human osteoblast cell line hFOB1.19 and OS cell lines. Then, we examined the effect of *APEX1* knockdown by a lentivirus-mediated small hairpin RNA (shRNA) on the proliferation of human OS cells both in vitro and in vivo, and bioinformatics analyses were performed to preliminarily explore the potential molecular mechanism underlying the role of *APEX1* in OS cell proliferation.

Materials and Methods

Specimens of osteosarcoma tissues and paracancerous tissues

Paired samples of human OS tissues and paracancerous tissues (subsequently used in RT-qPCR) were obtained by surgical procedures from eleven patients who were preoperatively pathologically diagnosed with OS at the First Affiliated Hospital of Guangxi Medical University. The research on human tissues was approved by the Ethical Committee of Guangxi Medical University, and informed consent was obtained from all patients and their immediate family members involved in this study. The human OS cell lines MG-63, HOS, Saos-2, U2OS; human osteoblast cell line hFOB1.19, and human renal epithelial 293T cells were purchased from the Cell Bank of Type Culture Collection of Chinese Academy of Sciences (Shanghai, China).

Real-time quantitative PCR

Total RNA was extracted from the tissues using TRIzol reagent. total RNA (1 μg from each specimen) was reverse-transcribed into cDNA with PrimeScript RT Master Mix, and 2 μl of the obtained cDNA was used as a template for PCR using SYBR Premix EX Taq. The primers used for PCR were as follows: *APEX1*-hF GTTTCTTACGGCATAGGCGAT, *APEX1*-hR CACAAAC

GAGTCAAATTCAGCC; *BCL2*-hF AGTACCTGAACCGGCACCT, *BCL2*-hR CCACACAAAC

CAAACTGAGCA; *Caspase3*-hF CATGGAAGCGAATCAATGGACT, *Caspase3*-hR CACAAAC

AGACCAGAGATGTCA; *p53*-hF GAGGTTGGCTCTGACTGTACC, *p53*-hR TCCGTCCAGTA

GATTAACCAAC; *CD31*-hF AACAGTGTGACATGAAGAGCC, *CD31*-hR TGAAAACAGCAC

G T C A T C C T T ; G A P D H - h F
TGACAACTTTGGTATCGTGGAAGG, GAPDH-hR
AGGCAGGG
ATGATGTTCTGGAGAG.

Construction of Lenti-shRNA vector, cell transfection, and APEX1 knockdown validation

The *APEX1*-siRNA sequence (5'-TGACAAAGAGGCAGCAGGA-3') was obtained from a previously published study [30], and the scramble sequence (TTCTCCGAACGTGTACGT) was used as a negative control (NC). The shRNA against *APEX1* was designed and synthesized by Shanghai Yunmi Biotechnology Co. Ltd. (Shanghai, China) on the basis of the aforementioned siRNA sequence, which was then inserted into the pGreenPuro vector using the restriction enzymes BamHI/EcoRI to obtain pGreenPuro-sh*APEX1*. Subsequently, pGreenPuro-sh*APEX1* was co-transfected into 293T cells with the lentiviral helper plasmids pSPAX2 and pMD2.G via Lipofectamine 2000. The lentivirus particles were stored at -80°C after purification and virus titer detection. The *APEX1*-shRNA or NC-shRNA lentivirus were separately used to transfect MG-63 cells according to the multiplicity of infection. To determine the lentiviral transfection efficacy in MG-63 cells, HEK293T cells with high affinity to lentivirus particles were set as a parallel control. At 3 days after transfection, the transfection efficacy of the recombinant lentivirus was determined using fluorescence microscopy. The *APEX1* knockdown efficacy of lentivirus was detected using RT-qPCR.

Western blot

MG-63 cells transfected with *APEX1*-shRNA and NC-shRNA plasmids, respectively, were harvested and lysed with RIPA lysis buffer for 30 min on ice. The lysates were centrifuged at 10000–14000 rpm at 4°C for 10 min, and then the supernatants were used to determine the protein concentration using the BCA Protein Assay Kit. Next, 30 µg protein from each specimen was separated using 10% sodium dodecyl sulfate–polyacrylamide gel electrophoresis and transferred onto polyvinylidene difluoride (PVDF) membranes. The PVDF membranes were blocked in skimmed milk for 1–2 h at room temperature and then incubated with rabbit anti-*APEX1* antibody (1:800) or anti-GAPDH antibody (1:10000) overnight at 4°C, followed by incubation with goat anti-mouse IgG antibody (1:5000) at 37°C for 2 h. The ECL Kit was used to perform the enhanced chemiluminescence assay.

MTT assay and xenograft tumor growth

MG-63 cells were collected at 10 days after stable transfection with *APEX1*-shRNA or NC-shRNA lentivirus and cultured in 96-well plates at 2×10^3 cells per well at 37°C with 5% CO₂ for 5 days. Next, 10 µl MTT (5 mg/ml) was added per well, and the cells were incubated in the dark for 4 h. Subsequently, the medium was removed, and 100 µl DMSO was added to each well. The proliferative potential of MG-63 cells was determined by measuring the optical density at 490 nm using a microplate reader.

The mouse experiments were approved by the Ethics Committee of Guangxi Medical University. Ten female specific-pathogen-free BALB/C nude mice aged 4–6 weeks (obtained from Shanghai Slack Laboratory Animal Co. Ltd., Shanghai, China) were divided into two groups of five mice each, which were subcutaneously injected with 100 µl of 1×10^8 /ml MG-63 cells stably transfected with *APEX1*-shRNA and NC-shRNA lentivirus, respectively, in the right underarm area. Tumor size was measured once a week since the second week after injection, and tumor volume was calculated based on length (y) and width (x) as follows: $x^2y/2$ (where $x < y$). The mice were euthanized after 5 weeks, and the tumors were resected and weighed. The rate of tumor inhibition due to *APEX1* knockdown was determined on the basis of tumor weight and volume, using the equation $(1 - a/b) \times 100\%$, where “a” represents the mean of tumor weight or the mean of volume in the *APEX1*-shRNA group of mice, and “b” represents the mean of tumor weight or the mean of volume in the NC-shRNA group of mice.

Hematoxylin–eosin staining and immunohistochemistry

Tumor tissues obtained from the *APEX1*-shRNA and NC-shRNA groups were fixed in 4% paraformaldehyde for 24 h and placed in processing cassettes after rinsing with distilled water for 30 min. The tissues were dehydrated in gradient ethanol and embedded in paraffin wax blocks. Next, the tissue sections with a thickness of 4 µm were dewaxed in xylene, rehydrated by passing through an ethanol gradient of decreasing concentrations and washed with distilled water, followed by staining with hematoxylin and eosin (HE). For immunohistochemistry (IHC), the fixation, dehydration, embedding, and sectioning of tumor tissues were performed in the same manner. The paraffin-embedded tumor tissue sections were soaked in xylene and gradient ethanol for dewaxing. Heat-mediated antigen retrieval was performed with citrate buffer (pH 6.0) for 10 min. The sections were treated with 3% H₂O₂ methanol for 15 min to quench endogenous peroxidase activity and then incubated in goat serum (1:10) at 37°C for 1 h to block non-specific binding sites. Rabbit anti-*CD31* antibody (1:500) was added on top of the sections, following which they were incubated overnight at 4°C; then, the sections were incubated at room temperature for 30 min. The horseradish peroxidase-conjugated secondary antibody (anti-rabbit IgG [H+L], 1:1000) was added, and the sections were incubated at 37°C for 30 min. DAB was used as a chromogenic agent, and hematoxylin was used to counterstain the nucleus for 30 s. The tissue sections were observed under a microscope.

Terminal deoxynucleotidyl transferase dUTP nick end labeling assay

For the terminal deoxynucleotidyl transferase dUTP nick end labeling (TUNEL) assay, the fixation, dehydration, embedding, and sectioning of the tumor tissues was performed in the same manner as for HE staining. After dewaxing the sections, a circle was drawn around the tissue with a PAP pen. Protease K working solution (1:9) was added to the sections, and the sections were incubated at 37°C for 22 min, after which they were

washing thrice with phosphate-buffered saline (PBS) in a decolorization shaker. The tissues were then incubated with a membrane-breaking solution (1:1000) at room temperature for 20 min, followed by incubation at room temperature with buffer. The tissue sections covered with the reaction mixture (TDT enzyme: dUTP: buffer = 1:5:50) were incubated in a wet box at 37°C for 2 h. The sections were washed with PBS, and DAPI Fluoromount-GTM was used for nuclear staining and sealing. The sections were observed and imaged using fluorescence microscopy.

Transcription factor prediction and gene enrichment analysis

TFs involved in the transcriptional regulation of *APEX1* were predicted on the basis of three databases: TRRUST (<https://www.grnpedia.org/trrust/>), TRED (<http://rulai.cshl.edu/TRED>) and TransFac (<http://gene-regulation.com/pub/databases.html>). A PPI network was constructed by retrieving high-confidence protein-protein interaction pairs from STRING database (<http://string-db.org/>), in which the PPI combined score >0.9 was set as the screening criterion, to identify proteins that interact with *APEX1*. Gene ontology (GO) terms and Kyoto Encyclopedia of Genes and Genomes (KEGG) pathway enrichment analysis of the set of *APEX1*-related genes were performed using DAVID tools (<https://david.ncifcrf.gov/>). GO terms or KEGG pathways were considered as being significantly enriched, when the number of enriched genes was ≥ 2 at $P < 0.05$.

Statistical Analysis

Student's t-test was used for comparing quantitative data among groups, Chi-square test and Fisher's exact test was used to analyze qualitative data. Mann-Whitney U test was used to compare the volume and weight of tumors. All statistical analyses were performed using the SPSS 22.0 software package and GraphPad prism 5.0. $P < 0.05$ was considered to indicate statistical significance.

Results

APEX1 is highly expressed in osteosarcoma tissues

To investigate the effect of *APEX1* expression difference

on OS cells, we first determined the transcript levels of *APEX1* in human OS tissues and paracancerous tissues using RT-qPCR. The data showed that *APEX1* mRNA was upregulated in 6/11 (54.54%), not significantly different in 3/11 (27.27%) and downregulated in 2/11 (18.19%) of the OS tissues compared with the paracancerous tissues (Figure 1A). The results indicate that *APEX1* expression is significantly increased in OS (Figure 1B, $P = 0.035$).

APEX1 expression in human osteosarcoma cells and hFOB1.19 cells and lentivirus-mediated small hairpin RNA significantly knocks down *APEX1* expression

The mRNA levels of *APEX1* in the human osteoblast cell line hFOB1.19 and human OS cell lines MG-63, HOS, Saos-2, U2OS were determined using RT-qPCR. Compared with human osteoblast hFOB1.19 cells, human OS cell lines showed significantly higher *APEX1* mRNA expression levels, with the highest level of expression observed in MG-63 cells (Figure 2A). To assess the impact of *APEX1* knockdown on OS cell proliferation, lentivirus-mediated shRNA against *APEX1* was transfected into MG-63 cells. As shown in Figure 2B, the mRNA level of *APEX1* in MG-63 cells transfected with the *APEX1*-shRNA lentivirus was 72.4% lower ($P = 0.003$) than in those transfected with the NC-shRNA lentivirus and 77.8% lower ($P = 0.001$) than in the blank control, but no significant difference was found between the NC-shRNA group and the blank control ($P = 0.167$). *APEX1* protein expression was also significantly lower in the *APEX1*-shRNA lentivirus group (Figure 2C and 2D, $P = 0.009$).

APEX1 knockdown suppresses MG-63 cell proliferation and induces cells apoptosis

To examine the effects of *APEX1* knockdown on OS cell proliferation in vitro, we detected the proliferative potential of MG-63 cells transfected with either *APEX1*-shRNA or NC-shRNA lentivirus for five consecutive days using the MTT assay. The MTT assay results revealed that the proliferation rate of MG-6 cells transfected with *APEX1*-shRNA lentivirus was slower than the proliferation rate of those transfected with NC-shRNA lentivirus (Figure 3A). In addition, to confirm whether these results could be replicated in vivo, a xenograft model of OS was established in nude mice by subcutaneous

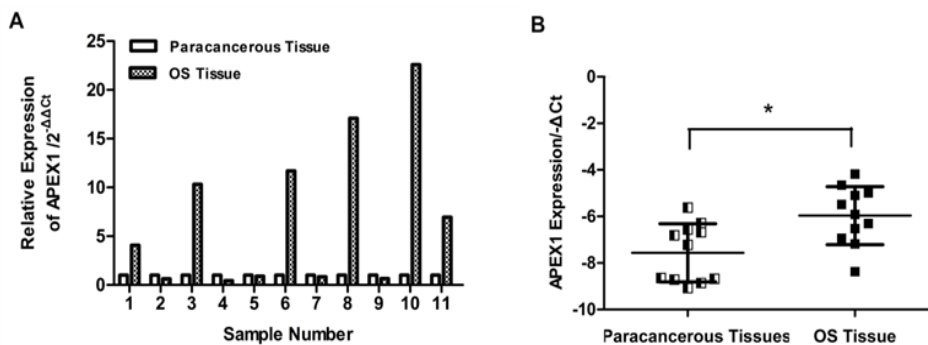


Figure 1. *APEX1* Expression was Detected Both in Tissues and Cell Lines (A) The expression levels of *APEX1* mRNA in 11 pairs of human OS tissues and paired paracancerous tissues. The expression difference in paired samples of No.1, No.2, No.3, No.4, No.6, No.8, No.10 and No.11 were statistically significant, but these of No.5, No.7 and No.9 have no statistical significance. (B) a significantly high expression of *APEX1* in OS tissues compared with paired paracancerous tissues (* $P=0.035$).

Table 1. Go Enrichment Analysis of the Genes in PPI Network. BP represents biological process, CC represents cellular component and MF represents molecular function.

| Category | GO-ID | Term | Count | PValue | FDR |
|----------|-------|--|-------|----------|----------|
| BP | 6297 | nucleotide-excision repair, DNA gap filling | 17 | 5.74E-37 | 8.23E-34 |
| BP | 722 | telomere maintenance via recombination | 17 | 4.63E-34 | 6.63E-31 |
| BP | 6284 | base-excision repair | 17 | 3.11E-33 | 4.45E-30 |
| BP | 6296 | nucleotide-excision repair, DNA incision, 5'-to lesion | 15 | 1.23E-27 | 1.77E-24 |
| BP | 33683 | nucleotide-excision repair, DNA incision | 15 | 1.95E-27 | 2.79E-24 |
| BP | 42769 | DNA damage response, detection of DNA damage | 14 | 2.30E-25 | 3.29E-22 |
| BP | 6260 | DNA replication | 19 | 3.08E-25 | 4.41E-22 |
| BP | 19985 | translesion synthesis | 13 | 5.95E-23 | 8.52E-20 |
| BP | 6283 | transcription-coupled nucleotide-excision repair | 15 | 8.56E-23 | 1.23E-19 |
| BP | 42276 | error-prone translesion synthesis | 10 | 4.22E-19 | 6.04E-16 |
| CC | 5654 | nucleoplasm | 44 | 5.76E-31 | 5.77E-28 |
| CC | 5634 | nucleus | 41 | 4.38E-15 | 4.34E-12 |
| CC | 5663 | DNA replication factor C complex | 6 | 5.49E-13 | 5.50E-10 |
| CC | 43625 | delta DNA polymerase complex | 4 | 6.42E-08 | 6.43E-05 |
| CC | 8622 | epsilon DNA polymerase complex | 4 | 1.60E-07 | 1.61E-04 |
| CC | 31390 | Ctf18 RFC-like complex | 4 | 8.92E-07 | 8.94E-04 |
| CC | 784 | nuclear chromosome, telomeric region | 7 | 9.91E-07 | 9.93E-04 |
| CC | 43234 | protein complex | 8 | 8.26E-05 | 0.082798 |
| CC | 5667 | transcription factor complex | 6 | 1.35E-04 | 0.135442 |
| CC | 5739 | mitochondrion | 12 | 4.55E-04 | 0.455255 |
| MF | 3684 | damaged DNA binding | 15 | 6.66E-24 | 8.02E-21 |
| MF | 3677 | DNA binding | 31 | 2.94E-19 | 3.54E-16 |
| MF | 3887 | DNA-directed DNA polymerase activity | 9 | 7.87E-15 | 9.49E-12 |
| MF | 19104 | DNA N-glycosylase activity | 6 | 3.35E-11 | 4.03E-08 |
| MF | 5515 | protein binding | 46 | 4.27E-11 | 5.14E-08 |
| MF | 3690 | double-stranded DNA binding | 9 | 5.33E-11 | 6.42E-08 |
| MF | 19899 | enzyme binding | 13 | 8.02E-11 | 9.65E-08 |
| MF | 3689 | DNA clamp loader activity | 5 | 3.66E-09 | 4.41E-06 |
| MF | 4844 | uracil DNA N-glycosylase activity | 4 | 2.01E-07 | 2.43E-04 |
| MF | 35035 | histone acetyltransferase binding | 5 | 1.03E-06 | 0.001237 |

inoculation with MG-63 cells stably transfected with *APEX1*-shRNA or NC-shRNA lentivirus. As shown in Figure 3B, smaller tumors were found in mice receiving cells transfected with *APEX1*-shRNA. The transplanted tumors in the *APEX1*-shRNA group showed a remarkably

lower volume (Figure 3C, $P = 0.009$) and weight (Figure 3D, $P = 0.009$) than those in the NC-shRNA group. The volumetric and gravimetric inhibition rates were 75.17% and 58.1%, respectively (Figure 3E and 3F).

The HE staining results indicated that OS cells in the

Table 2. KEGG Pathway Enrichment Analysis of the Genes in PPI Network. Count represented the number of enriched genes

| KEGG-ID | Term | Count | PValue | FDR |
|----------|----------------------------|-------|----------|----------|
| hsa03410 | Base excision repair | 24 | 1.17E-47 | 1.17E-44 |
| hsa03030 | DNA replication | 19 | 5.34E-33 | 5.34E-30 |
| hsa03420 | Nucleotide excision repair | 18 | 4.61E-28 | 4.61E-25 |
| hsa03430 | Mismatch repair | 14 | 1.08E-24 | 1.08E-21 |
| hsa05166 | HTLV-I infection | 13 | 1.10E-08 | 1.10E-05 |
| hsa03440 | Homologous recombination | 7 | 1.13E-08 | 1.12E-05 |
| hsa00240 | Pyrimidine metabolism | 9 | 8.52E-08 | 8.51E-05 |
| hsa00230 | Purine metabolism | 9 | 5.98E-06 | 0.005974 |
| hsa03460 | Fanconi anemia pathway | 3 | 0.037704 | 31.87223 |

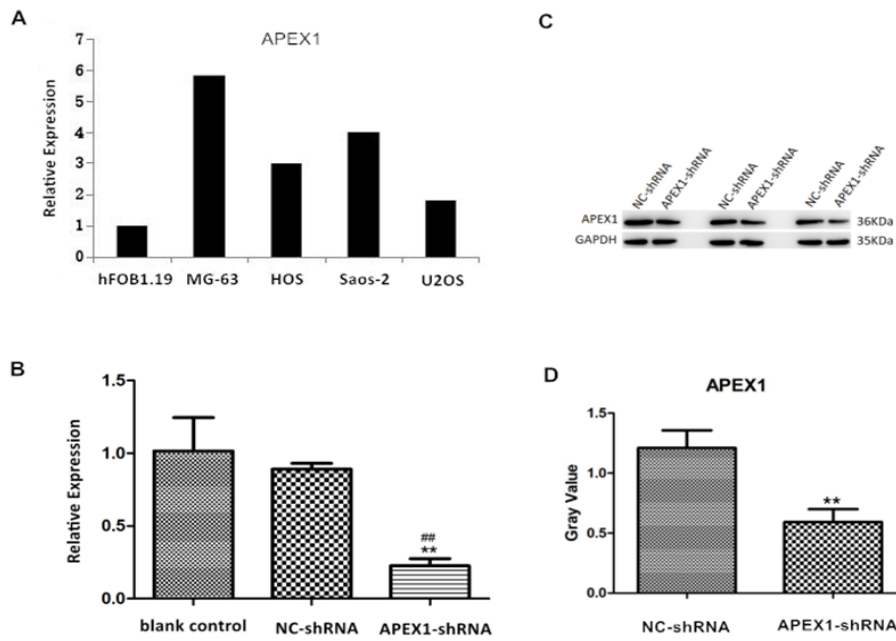


Figure 2. The Significant Knockdown of *APEX1* both in mRNA and Protein Levels. (A) *APEX1* mRNA levels in hFOB1.19 osteoblast cell line and human OS cell lines. (B) *APEX1* mRNA was significantly down-regulated in MG-63 cells of *APEX1*-shRNA group as compared to NC-shRNA group (** $P=0.003$) and blank control group (** $P=0.001$), while no significant difference between NC-shRNA group and blank control group ($P=0.167$). (C, D) *APEX1* protein down-regulation in MG-63 cells of *APEX1*-shRNA group, as compared to NC-shRNA group, were further confirmed by western blot (** $P=0.009$).

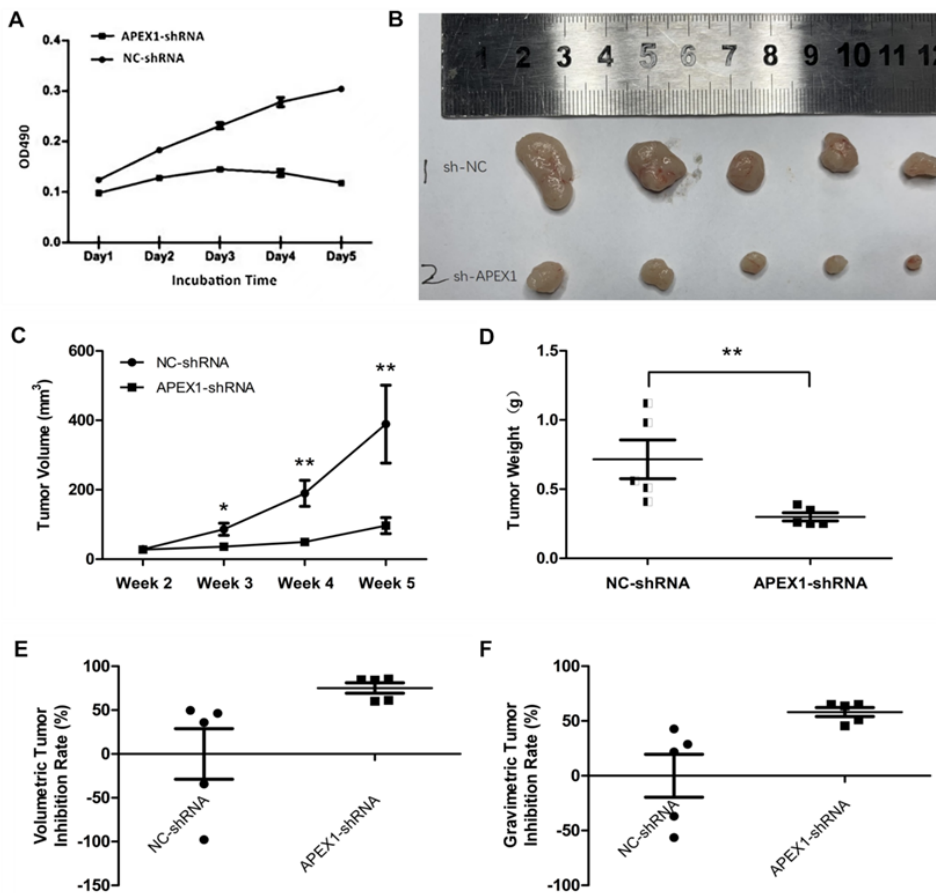


Figure 3. *APEX1* Knockdown Suppressed the Proliferation of MG-63 Cells and Xenograft Tumor Growth. (A) Knockdown of *APEX1* led to the proliferation inhibition of MG-63 cells in MTT assay. (B) *APEX1* knockdown suppressed the xenograft tumor growth. (C, D, E, F) Compared to NC-shRNA group, the inhibition rates of volume and weight in *APEX1*-shRNA group were 75.17% (** $P=0.009$) and 58.1% (** $P=0.009$).

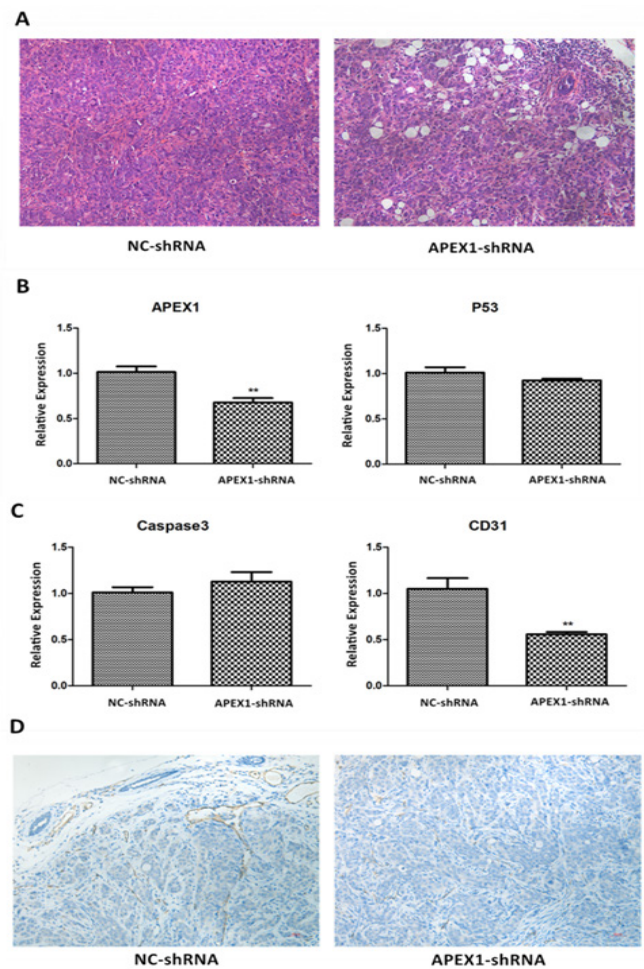


Figure 4. HE Stain of the Xenograft Tumor Tissues from the Two Groups and the Expression Change of Apoptosis- and Angiogenesis-Related Genes. (A) As shown in the figure, the tumor cells in NC-shRNA group had larger volumes, uneven in size, higher nucleo-plasma ratio, hyperchromasia nuclei and extremely common mitotic figures as compared to *APEX1*-shRNA group. (B, C) The expression of CD31 in *APEX1*-shRNA group was remarkably down-regulated due to *APEX1* silence compared with NC-shRNA group ($P < 0.01$), but no significant expression difference was found in P53 and Caspase3 between the two groups. (D) IHC further confirmed the down-regulation of CD31 protein due to *APEX1* silence.

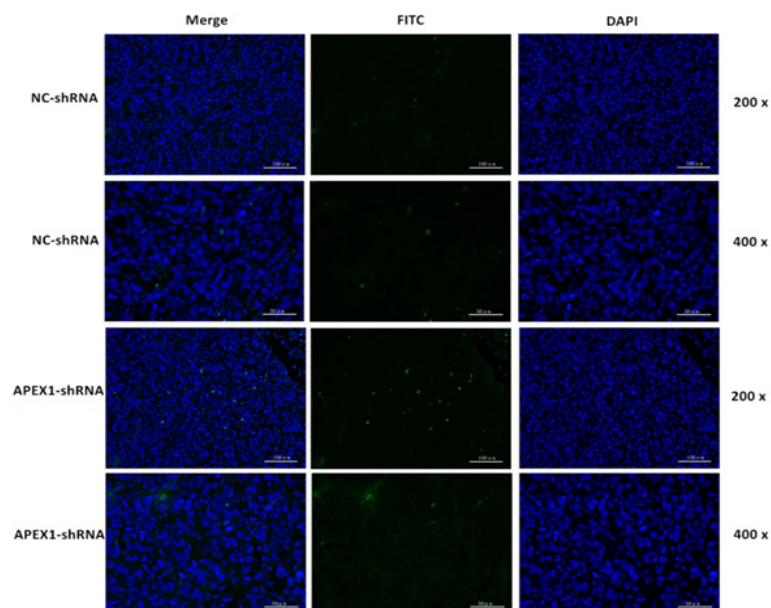


Figure 5. *APEX1* Knockdown Induced MG-63 Cells Apoptosis. The effect of *APEX1* knockdown on OS cells apoptosis was determined by TUNEL. Compared with NC-shRNA group, FITC green fluorescein labeled nuclei were increased in tumor cells of *APEX1*-shRNA group.

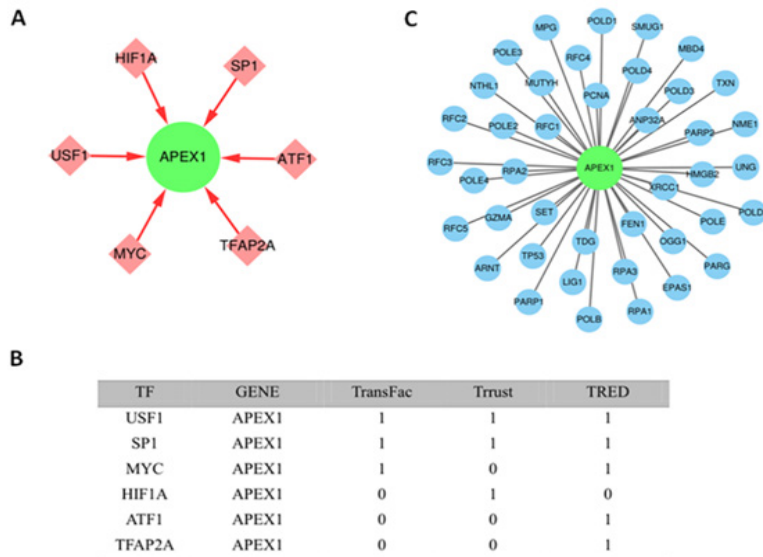


Figure 6. Transcriptional Regulatory Relationship and Protein-Protein Interaction Pairs. (A) The TFs that participate in the transcriptional control of *APEX1*. (B) 1 represents the regulatory relationships that exist in this database, 0 represents nonexistence. (C) The proteins interacted with *APEX1*.

NC-shRNA group had larger volumes, uneven size, a higher nucleus/cytoplasm ratio, hyperchromatic nuclei, and a higher frequency of mitotic figures than OS cells in the *APEX1*-shRNA group (Figure 4A). The RT-qPCR for nine paired tumor tissue samples showed that the expression of *APEX1* ($P = 0.0005$) and *CD31* ($P = 0.0007$) in the *APEX1*-shRNA group was significantly lower than that in the NC-shRNA group, but no differences were found for *p53* ($P = 0.169$) and Caspase3 ($P = 0.333$) expression in the two groups (Figure 4B). *BCL2* expression was not detected, likely owing to low abundance. IHC results confirmed that *CD31* is downregulated as a result of *APEX1* silencing (Figure 4C). The results of the TUNEL assay revealed that tumor tissues with *APEX1* knockdown had higher quantities of fluorescent expression (Figure 5). The above findings verified that *APEX1* knockdown in OS cells inhibited cell proliferation and promoted apoptosis.

Transcription factors involved in APEX1 regulation and enrichment of APEX1-related gene set

TF prediction based on the three databases indicated that six identified TFs particularly USF1 and SP1, which appeared in all databases were involved in the transcriptional regulation of *APEX1* (Figure 6A and 6B). The PPI network analysis suggested that 41 proteins interact with *APEX1* (Figure 6C). GO and KEGG enrichment analyses suggested that *APEX1* is mainly located in the nucleus and was associated with damaged DNA binding and nucleotide excision repair, indicating that it is involved in DDR (Table 1). In addition, *APEX1*-related gene set were also significantly enriched in the pathways related to DDR and nucleotide metabolism, the most enriched pathways of which included base excision repair (BER), nucleotide excision repair (NER), mismatch repair (MMR), and homologous recombination (HR; Table 2).

Discussion

The pathogenesis and progression of OS is complex and has not been fully elucidated to date. However, previous studies have demonstrated that it is associated with aberrations in genes related to certain tumorigenic pathways; regulators of proliferation, migration, invasion, cell cycle progression, apoptosis, angiogenesis, and osteoclast function; transcription factors; and miRNAs [31]. For instance, there is evidence that genomic alterations in the PI3K/mTOR pathway were associated with multiple pathological processes of OS [32]. Upregulation of VEGF pathway genes was reported to be significantly associated with microvascular density and tumor-free survival in OS [33]. The Wnt signaling pathway is indispensable for osteoblast lineage determination, whereas aberrant components of the Wnt pathway facilitate the development and progression of OS [34]. In addition, OS pathogenesis and progression have also been associated with the inactivation of *p53*, *Rb*, and *WWOX* as well as upregulation of *APEX1*, *Myc*, *RECQL4*, and *RPL8* [35]. Notable among these proteins is *APEX1*, the C-terminal region of which is involved in repairing DNA damage caused by ultraviolet radiation and ROS, whereas the N-terminal part exhibits redox activity.

The present findings confirmed that *APEX1* gene was upregulated in OS tissue samples in comparison with the paired paracancerous tissue samples. *APEX1* knockdown in MG-63 cells significantly suppressed cell proliferation and xenograft tumor growth, induced cell apoptosis, and reduced the expression of the proliferation-promoting gene *CD31*. The platelet endothelial cell adhesion molecule-1 (PECAM-1/*CD31*), which belongs to the immunoglobulin gene superfamily, is expressed on endothelial cells and plays an important role in angiogenesis, inflammation, integrin activation, and cell-cell adhesion [36-38]. Previous studies have shown that formation of metastatic

foci of OS cells in other bones is regulated by *CD31*, the expression of which facilitates the adhesion of OS cells to endothelial cells and transendothelial migration, which is mediated by homophilic interactions between *CD31* and *CD31* and heterophilic interactions between *CD31* and $\alpha\beta 3$ integrin [39]. However, there have been few reports about the role of *CD31* in OS proliferation. The present results suggest that *APEX1* facilitates the proliferation of OS cells via *CD31*. Nonetheless, the detailed molecular mechanism through which *APEX1* affects the proliferation of OS cells needs to be further elucidated. Here, we identified six TFs—USF1, SP1, MYC, HIF1A, ATF1, and TFAP2A—that are potentially involved in the transcriptional regulation of *APEX1* based on the three databases—TransFac, TRRUST, and TRED. Of particular note among these TFs are USF1 and SP1, which were identified in all three databases, suggesting that the two TFs are particularly likely to be involved in the transcriptional regulation of *APEX1*. USF1 is a multifunctional TF widely expressed in eukaryotes and plays an important role in glucolipid metabolism, melanin deposition, and cell proliferation. A previous study reported that USF1 induced the expression of lncRNA GAS6-AS2 (GAS6-AS2) by binding to its promoter, which enhanced its binding to miR-934 and led to the inhibition of miR-934 expression. Decreased expression of miR-934 enhanced the expression of BCAT1—associated with OS—which eventually facilitated the proliferation, migration, and invasion of OS cells and led to cell apoptosis inhibition. This finding indicates that the USF1/GAS6-AS2/miR-934/BCAT1 signaling axis likely mediates the modulation of malignant phenotypes of OS cells. Although the present findings suggest that USF1 is involved in the transcriptional regulation of *APEX1*, the USF1-binding site in the promoter of *APEX1* remains to be identified. Moreover, the GO enrichment analysis of the identified genes showed that *APEX1*-related genes, primarily localized in nucleus, were strongly associated with NER, BER, and telomere maintenance via recombination—known as alternative lengthening of telomeres—and involved in damaged DNA or protein binding as well as cell metabolism. Furthermore, KEGG pathway analysis showed that *APEX1* is mainly involved in DDR-related pathways including BER, NER, and MMR.

DDR is essential for chromosome stabilization and accuracy of DNA replication and transcription. There are four different types of DDR: BER, NER, MMR, and DNA double-strand break repair (DSBR)—which includes homologous recombination and non-homologous end joining [40]. The most important of these is BER, which is primarily responsible for the repair of DNA damage due to ROS, radiation, and chemotherapeutic agents. DDR is a multistep process, which needs to be initiated by sensors that have a tendency for binding to DNA lesions, transducers, and mediators to generate and amplify a damage-related signal for building a bridge between sensors and effectors. DNA damage intensity eventually determines whether damage repair or apoptosis is initiated [41]. Genetic alterations in DDR pathways, known as a vital mechanism for cancer progression, mainly

contribute to increased genetic mutation rate and cancer susceptibility [42] and are also considered to be potential therapeutic targets for OS, as various somatic alterations were identified in specimens from patients with OS [43]. Suppression of DDR pathway components such as *APEX1*, ERCC1, and EXO1 has been reported to decrease the resistance of OS cells to chemoradiotherapy [40]. Overexpression of N-methylpurine-DNA glycosylase (MPG), a sensor in the BER pathway, was demonstrated to be a potential therapeutic approach for increasing the sensitivity of OS cells to chemotherapy with DNA-damaging agents [44]. Moreover, a single nucleotide polymorphism in MPG was reported to be significantly associated with OS pathogenesis [45]. The BER pathway, in which *APEX1* plays a role, is crucial in the proliferation and resistance to chemoradiotherapy of malignant cells. As a sensor for BER, *APEX1*—together with AP endonuclease—is a key enzyme in the BER pathway; it binds to the AP sites arising from incorrect base excision by N-glycosylase to cut the damaged DNA single strand, which paves the way for base extension and DNA single-strand rejoining. However, more conclusive evidence is required to confirm whether USF1 or SP1 regulate *APEX1* transcription and whether it affects the interaction between *APEX1* and various OS-related factors such as *CD31* and the recruitment of *APEX1* in signal transduction related to OS cell proliferation.

Author Contribution Statement

Lu Yuyan and Luo Shuju carried out the experiments and wrote the main manuscript text. Lu Wen and Zheng Jie carried out the data processing and prepared the figures. All authors reviewed the manuscript.

Acknowledgements

This work was supported by Guangxi Medical University Youth Science Foundation project (GXMUYSF201803). We thank the medical science experiment center and animal experimental center of Guangxi Medical University for supplying laboratory equipments and technical support during the study.

Ethics approval and consent to participate

The research was approved by the Ethical Committee of Guangxi Medical University.

Patient consent for publication

Written informed consent was obtained from the patients for publication of OS tissue sample data in this research.

Competing interests

The authors declare no competing financial interests.

References

- Ottaviani G, Jaffe N. The epidemiology of osteosarcoma. *Cancer Treat Res*. 2009;152:3-13. https://doi.org/10.1007/978-1-4419-0284-9_1.

2. Siegel RL, Miller KD, Jemal A. Cancer statistics, 2018. *CA Cancer J Clin*. 2018;68(1):7-30. <https://doi.org/10.3322/caac.21442>.
3. Miller BJ, Cram P, Lynch CF, Buckwalter JA. Risk factors for metastatic disease at presentation with osteosarcoma: An analysis of the seer database. *J Bone Joint Surg Am*. 2013;95(13):e89. <https://doi.org/10.2106/jbjs.L.01189>.
4. Klein MJ, Siegal GP. Osteosarcoma: Anatomic and histologic variants. *Am J Clin Pathol*. 2006;125(4):555-81. <https://doi.org/10.1309/uc6k-qhld-9lv2-kenn>.
5. Kuijjer ML, Hogendoorn PC, Cleton-Jansen AM. Genome-wide analyses on high-grade osteosarcoma: Making sense of a genomically most unstable tumor. *Int J Cancer*. 2013;133(11):2512-21. <https://doi.org/10.1002/ijc.28124>.
6. Stephens PJ, Greenman CD, Fu B, Yang F, Bignell GR, Mudie LJ, et al. Massive genomic rearrangement acquired in a single catastrophic event during cancer development. *Cell*. 2011;144(1):27-40. <https://doi.org/10.1016/j.cell.2010.11.055>.
7. Taylor BS, Barretina J, Maki RG, Antonescu CR, Singer S, Ladanyi M. Advances in sarcoma genomics and new therapeutic targets. *Nat Rev Cancer*. 2011;11(8):541-57. <https://doi.org/10.1038/nrc3087>.
8. Junttila MR, de Sauvage FJ. Influence of tumour micro-environment heterogeneity on therapeutic response. *Nature*. 2013;501(7467):346-54. <https://doi.org/10.1038/nature12626>.
9. Evans AR, Limp-Foster M, Kelley MR. Going ape over ref-1. *Mutat Res*. 2000;461(2):83-108. [https://doi.org/10.1016/s0921-8777\(00\)00046-x](https://doi.org/10.1016/s0921-8777(00)00046-x).
10. Tell G, Quadrioglio F, Tiribelli C, Kelley MR. The many functions of ape1/ref-1: Not only a DNA repair enzyme. *Antioxid Redox Signal*. 2009;11(3):601-20. <https://doi.org/10.1089/ars.2008.2194>.
11. Bhakat KK, Mantha AK, Mitra S. Transcriptional regulatory functions of mammalian ap-endonuclease (ape1/ref-1), an essential multifunctional protein. *Antioxid Redox Signal*. 2009;11(3):621-38. <https://doi.org/10.1089/ars.2008.2198>.
12. Kelley MR, Georgiadis MM, Fishel ML. Ape1/ref-1 role in redox signaling: Translational applications of targeting the redox function of the DNA repair/redox protein ape1/ref-1. *Curr Mol Pharmacol*. 2012;5(1):36-53. <https://doi.org/10.2174/1874467211205010036>.
13. Kim JM, Yeo MK, Lim JS, Song IS, Chun K, Kim KH. Apex1 expression as a potential diagnostic biomarker of clear cell renal cell carcinoma and hepatobiliary carcinomas. *J Clin Med*. 2019;8(8). <https://doi.org/10.3390/jcm8081151>.
14. Tummanatsakun D, Proungvitaya T, Roytrakul S, Limpaboon T, Wongkham S, Wongkham C, et al. Serum apurinic/apyrimidinic endodeoxyribonuclease 1 (apex1) level as a potential biomarker of cholangiocarcinoma. *Biomolecules*. 2019;9(9). <https://doi.org/10.3390/biom9090413>.
15. Tummanatsakun D, Proungvitaya T, Roytrakul S, Proungvitaya S. Bioinformatic prediction of signaling pathways for apurinic/apyrimidinic endodeoxyribonuclease 1 (apex1) and its role in cholangiocarcinoma cells. *Molecules*. 2021;26(9). <https://doi.org/10.3390/molecules26092587>.
16. Sun Z, Chen G, Wang L, Sang Q, Xu G, Zhang N. Apex1 promotes the oncogenicity of hepatocellular carcinoma via regulation of map2k6. *Aging*. 2022;14(19):7959-71. <https://doi.org/10.18632/aging.204325>.
17. Peng L, Liu Y, Chen J, Cheng M, Wu Y, Chen M, et al. Apex1 regulates alternative splicing of key tumorigenesis genes in non-small-cell lung cancer. *BMC Med Genomics*. 2022;15(1):147. <https://doi.org/10.1186/s12920-022-01290-0>.
18. Yang JL. Investigation of osteosarcoma genomics and its impact on targeted therapy: An international collaboration to conquer human osteosarcoma. *Chin J Cancer*. 2014;33(12):575-80. <https://doi.org/10.5732/cjc.014.10209>.
19. Yang J, Yang D, Cogdell D, Du X, Li H, Pang Y, et al. Apex1 gene amplification and its protein overexpression in osteosarcoma: Correlation with recurrence, metastasis, and survival. *Technol Cancer Res Treat*. 2010;9(2):161-9. <https://doi.org/10.1177/153303461000900205>.
20. Jiang X, Shan J, Dai N, Zhong Z, Qing Y, Yang Y, et al. Apurinic/apyrimidinic endonuclease 1 regulates angiogenesis in a transforming growth factor β -dependent manner in human osteosarcoma. *Cancer Sci*. 2015;106(10):1394-401. <https://doi.org/10.1111/cas.12763>.
21. Ren T, Qing Y, Dai N, Li M, Qian C, Yang Y, et al. Apurinic/apyrimidinic endonuclease 1 induced upregulation of fibroblast growth factor 2 and its receptor 3 induces angiogenesis in human osteosarcoma cells. *Cancer Sci*. 2014;105(2):186-94. <https://doi.org/10.1111/cas.12334>.
22. Zhao Z, Lin X, Tong Y, Li W. Silencing lncrna zfas1 or elevated microrna-135a represses proliferation, migration, invasion and resistance to apoptosis of osteosarcoma cells. *Cancer Cell Int*. 2019;19:326. <https://doi.org/10.1186/s12935-019-1049-x>.
23. Liu Y, Zhang Z, Li Q, Zhang L, Cheng Y, Zhong Z. Mitochondrial ape1 promotes cisplatin resistance by downregulating ros in osteosarcoma. *Oncol Rep*. 2020;44(2):499-508. <https://doi.org/10.3892/or.2020.7633>.
24. Wang D, Zhong ZY, Li MX, Xiang DB, Li ZP. Vector-based ape1 small interfering rna enhances the sensitivity of human osteosarcoma cells to endostatin in vivo. *Cancer Sci*. 2007;98(12):1993-2001. <https://doi.org/10.1111/j.1349-7006.2007.00616.x>.
25. Xiao H, Jiang N, Zhang H, Wang S, Pi Q, Chen H, et al. Inhibitors of ape1 redox and atm synergistically sensitize osteosarcoma cells to ionizing radiation by inducing ferroptosis. *Int Immunopharmacol*. 2024;139:112672. <https://doi.org/10.1016/j.intimp.2024.112672>.
26. Liang W, Wei X, Li Q, Dai N, Li CY, Deng Y, et al. Microrna-765 enhances the anti-angiogenic effect of cddp via ape1 in osteosarcoma. *J Cancer*. 2017;8(9):1542-51. <https://doi.org/10.7150/jca.18680>.
27. Dai N, Qing Y, Cun Y, Zhong Z, Li C, Zhang S, et al. Mir-513a-5p regulates radiosensitivity of osteosarcoma by targeting human apurinic/apyrimidinic endonuclease. *Oncotarget*. 2018;9(39):25414-26. <https://doi.org/10.18632/oncotarget.11003>.
28. Liang W, Li C, Li M, Wang D, Zhong Z. Microrna-765 sensitizes osteosarcoma cells to cisplatin via downregulating ape1 expression. *Onco Targets Ther*. 2019;12:7203-14. <https://doi.org/10.2147/ott.S194800>.
29. Dai N, Zhong ZY, Cun YP, Qing Y, Chen C, Jiang P, et al. Alteration of the microrna expression profile in human osteosarcoma cells transfected with ape1 sirna. *Neoplasma*. 2013;60(4):384-94. https://doi.org/10.4149/neo_2013_050.
30. Fung H, Demple B. Distinct roles of ape1 protein in the repair of DNA damage induced by ionizing radiation or bleomycin. *J Biol Chem*. 2011;286(7):4968-77. <https://doi.org/10.1074/jbc.M110.146498>.
31. Gill J, Gorlick R. Advancing therapy for osteosarcoma. *Nat Rev Clin Oncol*. 2021;18(10):609-24. <https://doi.org/10.1038/s41571-021-00519-8>.
32. Zhang J, Yu XH, Yan YG, Wang C, Wang WJ. Pi3k/akt signaling in osteosarcoma. *Clin Chim Acta*. 2015;444:182-92. <https://doi.org/10.1016/j.cca.2014.12.041>.
33. Yang J, Yang D, Sun Y, Sun B, Wang G, Trent JC, et al. Genetic amplification of the vascular endothelial growth

- factor (vegf) pathway genes, including vegfa, in human osteosarcoma. *Cancer*. 2011;117(21):4925-38. <https://doi.org/10.1002/cncr.26116>.
34. Cai Y, Cai T, Chen Y. Wnt pathway in osteosarcoma, from oncogenic to therapeutic. *J Cell Biochem*. 2014;115(4):625-31. <https://doi.org/10.1002/jcb.24708>.
 35. Yang J, Zhang W. New molecular insights into osteosarcoma targeted therapy. *Curr Opin Oncol*. 2013;25(4):398-406. <https://doi.org/10.1097/CCO.0b013e3283622c1b>.
 36. Muller WA, Weigl SA, Deng X, Phillips DM. Pecam-1 is required for transendothelial migration of leukocytes. *J Exp Med*. 1993;178(2):449-60. <https://doi.org/10.1084/jem.178.2.449>.
 37. Buckley CD, Doyonnas R, Newton JP, Blystone SD, Brown EJ, Watt SM, et al. Identification of alpha v beta 3 as a heterotypic ligand for cd31/pecam-1. *J Cell Sci*. 1996;109 (Pt 2):437-45. <https://doi.org/10.1242/jcs.109.2.437>.
 38. Dejana E, Zanetti A, Del Maschio A. Adhesive proteins at endothelial cell-to-cell junctions and leukocyte extravasation. *Haemostasis*. 1996;26(Suppl 4):210-9. <https://doi.org/10.1159/000217301>.
 39. Arihiro K, Inai K. Expression of cd31, met/hepatocyte growth factor receptor and bone morphogenetic protein in bone metastasis of osteosarcoma. *Pathol Int*. 2001;51(2):100-6. <https://doi.org/10.1046/j.1440-1827.2001.01164.x>.
 40. Sadoughi F, Maleki Dana P, Asemi Z, Yousefi B. DNA damage response and repair in osteosarcoma: Defects, regulation and therapeutic implications. *DNA Repair (Amst)*. 2021;102:103105. <https://doi.org/10.1016/j.dnarep.2021.103105>.
 41. Georgoulis A, Vorigias CE, Chrousos GP, Rogakou EP. Genome instability and yh2ax. *Int J Mol Sci*. 2017;18(9):1979. <https://doi.org/10.3390/ijms18091979>.
 42. Jackson SP, Bartek J. The DNA-damage response in human biology and disease. *Nature*. 2009;461(7267):1071-8. <https://doi.org/10.1038/nature08467>.
 43. Chen X, Bahrami A, Pappo A, Easton J, Dalton J, Hedlund E, et al. Recurrent somatic structural variations contribute to tumorigenesis in pediatric osteosarcoma. *Cell Rep*. 2014;7(1):104-12. <https://doi.org/10.1016/j.celrep.2014.03.003>.
 44. Wang D, Zhong Z-y, Zhang Q-h, Li Z-p, Kelley MR. Effect of adenoviral n-methylpurine DNA glycosylase overexpression on chemosensitivity of human osteosarcoma cells. *Zhonghua Bing Li Xue Za Zhi*. 2006;35(6):352-6.
 45. Mirabello L, Yu K, Berndt SI, Burdett L, Wang Z, Chowdhury S, et al. A comprehensive candidate gene approach identifies genetic variation associated with osteosarcoma. *BMC Cancer*. 2011;11(1):209. <https://doi.org/10.1186/1471-2407-11-209>.



This work is licensed under a Creative Commons Attribution-Non Commercial 4.0 International License.